

# Rework Process Window and Microstructural Analysis for Lead-Free Mirrored Bga Design Points

Matthew Kelly, Mitchell Ferrill  
IBM Corporation

Polina Snugovsky, Rupen Trivedi, Gaby Dinca, Chris Achong, Zohreh Bagheri  
Celestica International Inc.

## Abstract

Hot gas rework of BGAs with a mirrored BGA design configuration using SnAgCu based lead-free alloys is more challenging as compared to conventional SnPb techniques. Rework of BGAs using a conventional SnPb alloy system has historically required that mirrored BGA solder joints remain below the eutectic melt temperature of 183°C to avoid secondary (or partial) reflow of these mirrored solder joints. This requirement was traditionally established to maximize second level solder joint reliability performance of mirrored BGA devices. However, with the migration to SnAgCu based alloys, the approach of ensuring that mirrored BGA device solder joints also remain below the SnAgCu melting point (217°C) during hot gas rework operations presents a more difficult challenge. Increased conductive heat transfer rates through the printed circuit board (PCB) along with increased thermal exposures to adjacent surface mount components are impacts of elevated processing temperatures associated with the use of lead-free solders. As a result, secondary reflow of mirrored BGA solder joints is sometimes unavoidable – especially for thin PCB cross sections, ranging nominally from 0.050” to 0.062” (1.2 to 1.6mm).

The intent of this paper is to recommend changes in assembly materials and the process itself during hot gas rework of lead-free BGAs with a mirrored BGA configuration. The metallurgical analysis of final solder joint structures and the reliability performance of fully reflowed mirrored BGA devices will be reported. An eight month development effort indicates that mirrored SnAgCu BGA solder joints should be allowed to fully reflow when it is not possible to prevent mirrored solder joints from reaching onset melting (pasty range) temperatures. Thermo-mechanical solder joint reliability has shown improvement when these joints are processed above the alloy pasty range; when all attempts to remain below this range have been exhausted.

**Key words:** Lead-free hot gas rework, mirrored BGA designs, process development, halide-free flux, pasty range, metallurgical analysis, temperature sensitive components, thermo-mechanical reliability.

## Introduction

As printed circuit board assembly (PCBA) designers continue to increase electronic component population densities on PCBs, mirrored BGA design configurations are becoming more prevalent. Designers are constantly looking to fit more components into smaller double-sided card layouts. During the assembly process, if a lead-free BGA device on such a mirrored BGA layout requires rework, a hot gas rework operation may be required. This process, although similar to standard SnPb eutectic processing, requires much more attention to detail and process accuracy. Therefore, rework of a lead-free BGA with a mirrored BGA device is likely considered the most complex case for hot gas rework processing.

As shown in Figure 1, a mirrored BGA design construction consists of a BGA device on the top side of the printed circuit board assembly, with another BGA device on the bottom side of the assembly – directly under the top side device. The more rigid double sided construction is consequently more process sensitive and may exhibit lower thermo-mechanical reliability performance if specific material and process details are not carefully monitored and controlled.

Firstly, as shown in Figures 1 and 2, during hot gas rework of a mirrored BGA device it is important to thermally monitor the rework site of interest as well as the local PCB temperature, mirrored BGA solder joints under the rework site, any adjacent (same side) BGA solder joints, and any local temperature sensitive component (TSC) body temperatures.

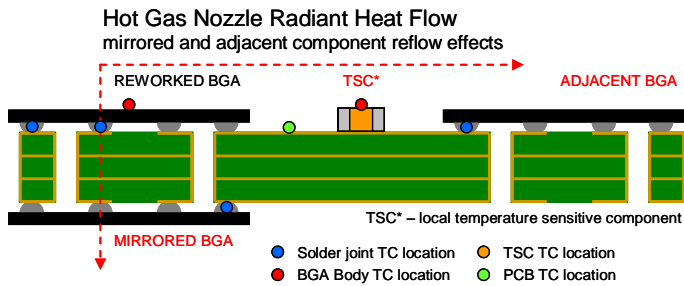


Figure 1. Mirrored, Adjacent, PCB, and TSC Heat Effects (not to scale)

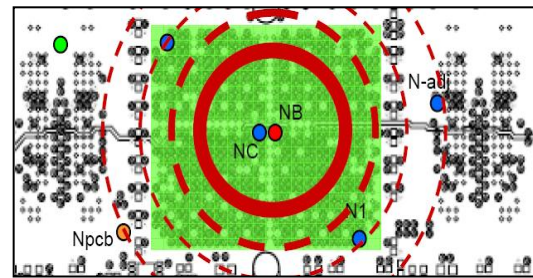


Figure 2. Hot Gas Nozzle Radial Heat Flow

Increased monitoring and measurement accuracy of these identified locations are important for several reasons:

- PCB reliability concerns such as delamination, inner layer separation, and/or Conductive Anodic Filament (CAF) growth may arise if excessive temperatures and time at temperatures are reached during the rework process. This damage can create undesired electrical pathways within the laminate.
- Final microstructure and formation of mirrored BGA solder joints will determine the longer term reliability performance of these solder joints after the rework process.
- Partial reflow of adjacent BGA solder joints can cause solidification anomalies such as shrinkage voids between the pad and solder or irregular shaped solder joints; thus degrading the reliability performance.
- Temperature sensitive components near the rework site may violate maximum temperature and/or time at temperature ratings, thus increasing the risk for latent field defects at these components on the rework assembly. [1]

Secondly, as shown in Figure 2 with the concentric red circles, there is an increased thermal radius from the rework nozzle location due to the elevated melting point of the SnAgCu alloy. With higher processing temperatures there is greater heat transfer from the top to bottom side of the assembly, and there is a larger thermal radius affecting adjacent components near the repair location. Since the heat transfer through the PCB is substantial, shielding the mirrored BGA from secondary reflow is of greater difficulty. Likewise, with a larger thermal radius, more adjacent BGAs and local TSCs will be affected, and must also be shielded to avoid partial reflow conditions. These highlighted issues are especially of concern for thinner card cross sections ranging nominally from 0.050" to 0.062" (1.2 to 1.6mm).

Thirdly, the conversion from SnPb to lead-free assembly has also required flux chemistry changes. Traditionally, for many high reliability SnPb products, water soluble flux chemistries were often used. The primary benefits of this selection were to maximize complex assembly process windows, and improve overall first pass yields. Any risks associated with un-activated (high activity) flux remaining after rework processing were negligible since the conventional process included a final washing operation – thus, removing any flux residues that may have remained. With the change to lead-free electronic card assembly, a shift to no-clean flux chemistries has also occurred. As a result, PCBAs that have been traditionally built using water soluble flux chemistries and were washed after assembly and rework steps *are no longer being washed*. The main issue with this conversion is that some processes, such as BGA mirrored rework, were built around the assumption that final assemblies would be washed after the repair was completed. Consequently, flux material selection, flux application formats, and site redress methods for initial lead-free processes were all developed based on this obsolete assumption.

Many no-clean lead-free flux formulations that are sold on the market and are used in production today are halide bearing (L1 type) fluxes [2]. These flux materials can pose significant reliability risks if not sufficiently controlled and activated during no-clean lead-free mirrored BGA rework operations. Dendritic growth, which can lead to conductor shorting, can be of considerable concern and may even lead to product failure in the field. Therefore, it is critical to eliminate this risk when performing mirrored BGA rework operations on high complexity, high reliability PCBAs through a change in the flux type and application method to ensure no-clean fluxes are thermally activated.

### Technical Issue Synopsis

Dendritic growth, leading to conductor shorting, was observed under *mirrored* SAC305  $\mu$ BGA test devices, after hot gas rework processing was conducted on a *topside* SAC305 BGA and  $\mu$ BGA locations. The mirrored BGA device was originally not allowed to reflow and a no-clean, halide bearing (L1 type) tack flux was used for the hot gas rework process. The results are shown below in Figures 3 and 4. Figure 3 shows the mirrored  $\mu$ BGA device location after the device was removed. Under the mirrored location, excessive flux pooling and charring was observed. Figure 4 shows upon closer examination that dendritic growth between via and pad structures on the PCB surface had occurred, ultimately resulting in device failure.



**Figure 3 (left). Figure 4 (right).** Dendritic Growth photos under a Mirrored  $\mu$ BGA Rework Location

### Root Cause of Failure

Failure analysis determined that the root cause of the test failure could be attributed to the flux chemistry used, the flux application method used, and inadequate thermal activation of the flux during the hot gas rework process.

Specifically, the failure resulted from:

- Excessive, uncontrolled usage of tack flux
- Use of halide containing flux chemistry
- Flux wicking down vias (card plated through holes) to underside BGA locations
- Avoidance of mirrored BGA secondary reflow
- Un-activated flux pooling under mirrored BGA devices
- Open via construction design between bottom side and top side BGAs
- Dendritic growth under electrical bias and humidity

The failure mechanism was determined to have multiple steps and is described below:

1. Halide bearing, no-clean tack flux was smeared into top side vias during the site redress process step, and was not removed before the reflow process.
2. As the replacement top side BGA and  $\mu$ BGA devices were being soldered, the excess tack flux, through capillary action and heat, wicked down the open via structures associated with the mirrored  $\mu$ BGA construction and pooled between the bottom side of the PCB and the backside  $\mu$ BGA device.
3. Traditional hot gas rework techniques were originally used to ensure that the mirrored  $\mu$ BGA solder joints did not undergo secondary reflow.
4. Partially un-activated halide bearing flux (only partially cured) pooled under the mirrored  $\mu$ BGA device.
5. No final wash step was used.
6. Over time, under electrical bias and ambient humidity, dendritic growth occurred.

Below in Figure 5, the failure mechanism is outlined graphically step by step.

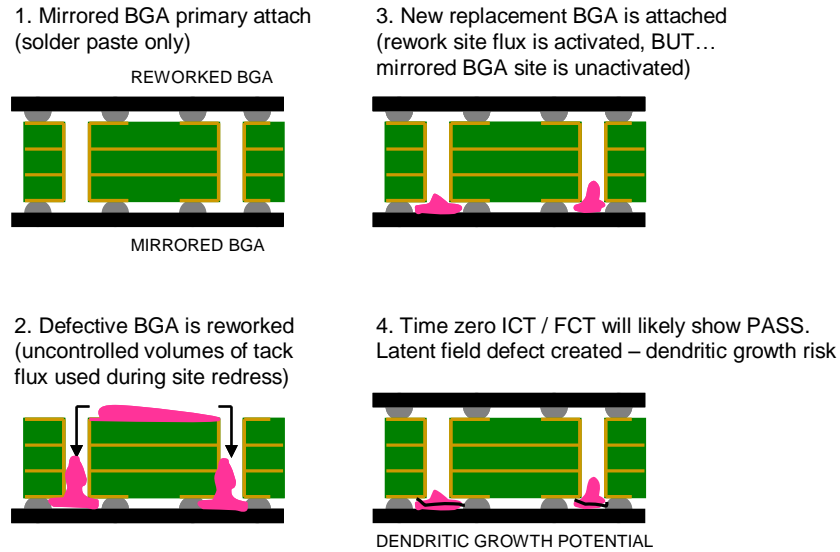


**Figure 5.** Mirrored  $\mu$ BGA Rework Dendritic Growth Pathway

### Intent and Objectives

With the observations of dendritic growth and resultant device failure, subsequent process development and qualification activities were initiated to improve the materials and process used for high complexity, high reliability lead-free mirrored BGA rework processing.

There were four main objectives of this process development activity. They included:

- Minimize the risk for dendritic growth resulting from un-activated no-clean lead-free fluxes during mirrored BGA rework processing.
- Develop a new manual rework process that minimized dendritic growth risks; optimizing assembly materials and processes for use with BGA devices – 0.5mm through 1mm pitch ranges.
- Test and analyze the new rework process using a suite of accelerated reliability environmental tests including accelerated thermal cycling, temperature/humidity/with bias, high temperature storage, torque/shock/vibration mechanical exposures, and time zero construction analysis.
- Examine final solder joint metallurgical structures for reworked and mirrored BGA locations to ensure sufficient metallurgical bonding had occurred.

### Material Selection and Process Development

A combination of optimized materials and process development activities were undertaken to minimize dendritic growth risks and are discussed below.

#### Material Selection

Rosin based flux systems are commonly used for high complexity, high reliability printed circuit board assembly. Many assemblers prefer to use ROL1 type flux systems as shown in Table 1. These flux systems by definition are allowed to contain < 0.5wt % of free halide (flux solids content). Even though the free halide content is low, there is *still reactive halide present* in these formulations after reflow, which can subsequently react with copper under electrical bias and humidity [3, 4] – if the flux is insufficiently activated. ROL0 type fluxes on the other hand, must contain 0.0wt % free halide (by definition) and therefore eliminate the risk of potential dendritic growth, even if the flux system is only partially activated during the assembly or rework process. Therefore, a migration to a halide-free (L0) type flux was implemented in this case.

**Table 1. J-STD-004 Flux Identification System Table [2]**

Materials of Composition <sup>2</sup>	Flux/Flux Residue Activity Levels	% Halide <sup>3</sup> (by weight)	Flux Type <sup>3</sup>	Flux Designator
Rosin (RO)	Low	0.0%	L0	ROL0
		<0.5%	L1	ROL1
	Moderate	0.0%	M0	ROM0
		0.5-2.0%	M1	ROM1
	High	0.0%	H0	ROH0
		>2.0%	H1	ROH1

The flux delivery method during hot gas rework site redress was another key area of the material selection activity. For (non-mirrored) BGA hot gas rework operations, tack flux is typically used during the site redress portion of the process. The main benefits of using this flux format during traditional site redress include improved delivery and control of the flux. The use of tack flux is often used to help reduce flooding and excess flux seepage under nearby components. Tack flux is generally applied with a small spatula and smeared across the entire BGA rework site. The high viscosity of tack flux acts to clean the site and maximize flux control during the site redress process. Although this process works very well for (non-mirrored) BGA rework operations, it does, however, pose problems with mirrored BGA configurations. As previously described in Figure 5, the use of tack flux during mirrored BGA rework site redress operations can lead to flux wicking down open via structures where it may not be sufficiently thermally activated during the hot gas reattachment process, and will increase the risk of dendritic growth during field life. As a result, a change from tack flux to controlled delivery of liquid flux, via a flux pen, was implemented in this case.

Lastly, cleaning agent improvements were implemented to properly clean the BGA site after redress operations. Conventional solvents such as isopropyl alcohol have typically been used after site redress operations, but were found to be inadequate to clean lead-free no-clean flux residues. Therefore a new flux cleaning chemistry was implemented.

In summary, the following assembly material changes were made to minimize dendritic growth risks associated with mirrored BGA no-clean lead-free hot gas rework operations:

- Switched from L1 to L0 (halide free) no-clean flux chemistry
- Prohibited usage of tack flux for mirrored BGA constructions; implemented the use of a liquid flux pen only
- Application of mini stencil and liquid flux (controlled application)
- Improved cleaning chemistry; migration away from IPA

### Rework Process Development

In combination with assembly material selection activities, an end-to-end review was conducted on the existing mirrored BGA hot gas rework process to examine opportunities for improvement and risk mitigation. Figure 6 shows the conventional process flow, along with highlighted steps (4 through 9) that were modified during process development activities.

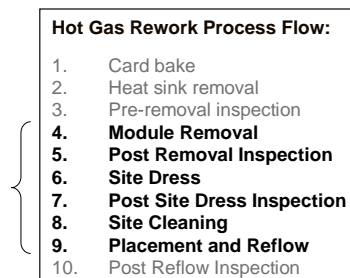


**Figure 6. Process Development Areas**

Changes were made in the module removal, inspection, site redress, cleaning, and reflow processes. Of these process changes, the most significant development activities involved final hot gas reflow.

The number of thermocouples used to monitor the mirrored lead-free BGA rework process was increased. Thermocouples should be placed in the following locations to ensure that the various components of the PCBA are sufficiently monitored and controlled (see Figure 1):

- Local PCB locations
- Adjacent components (same side devices)
- Temperature Sensitive Component bodies
- Mirrored BGA solder joints

During profile development, numerous profile iterations were conducted to ensure an optimized rework process window. Table 2 shows example optimized maximum peak temperatures and time above liquidus (TAL) measurements obtained after significant process development efforts. In Figure 1, general thermocouple locations are shown. Additional thermocouples located throughout the BGA interconnect field may be required to adequately characterize thermal gradients.

**Table 2. Maximum Peak Temperatures and TAL Times for various trial reflow profiles**

TC	TC Location	BGA 1		BGA 2		BGA 3	
		Max Peak (deg C)	TAL (sec)	Max Peak (deg C)	TAL (sec)	Max Peak (deg C)	TAL (sec)
1	Trigger	156	0	100	0	145	0
2	Rework BGA centre joint	238	76	238	97	238	79
3	Rework BGA corner joint	236	69	233	77	235	69
4	Rework BGA body	240	84	240	111	235	75
5	Mirrored BGA centre joint	232	61	231	73	213	0
6	Adjacent BGA corner joint	211	0	212	0	190	0
7	Local PCB	224	30	225	50	229	54

Resultant observations include:

- All temperature sensitive components were within maximum peak and TAL ranges
- A maximum PCB temperature of 245°C was maintained across all profiles
- The minimum solder joint temperature was maintained above 230°C
- Adjacent component solder joints remained below SnAgCu m.p. of 217°C
- Mirrored solder joint temperatures spanned the alloy’s melting point and pasty range

Figure 7 shows the same data graphically. Depending upon the design configuration, mirrored BGA solder joints may remain above 230°C (desired condition), may reflow within the pasty range of the solder, or may remain below 217°C and not reflow.

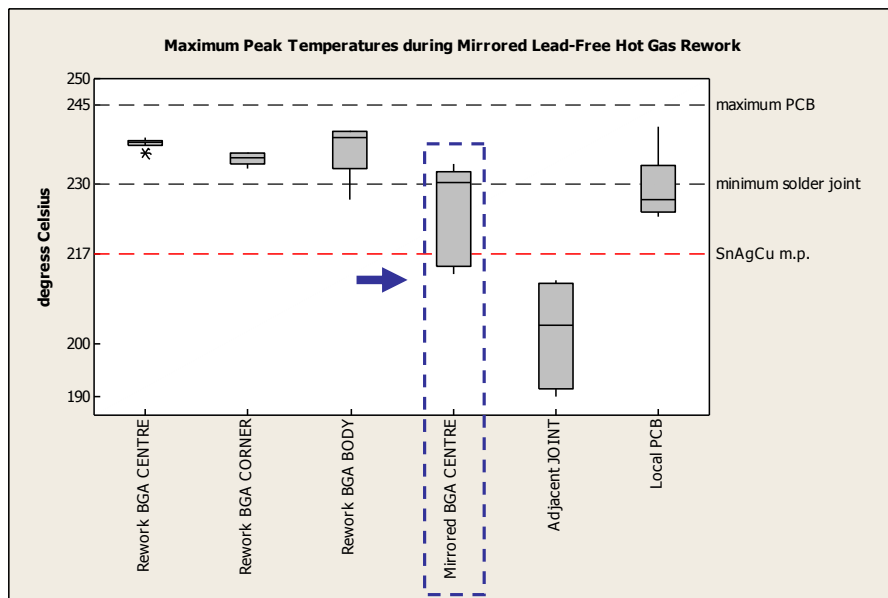


**Figure 7. Maximum Peak Temperature Ranges for Mirrored BGAs**

As will be discussed further in the following sections, significant rework process development activities have highlighted that lead-free mirrored solder joint temperatures during rework should be processed avoiding the alloy’s pasty range; allowing mirrored joints to fully reflow if they cannot be sufficiently shielded and remain below the melting point of the alloy.

## Metallurgical Analysis

In this study, hot gas rework profiles were created for two ball grid array components; (1) a  $\mu$ BGA and (2) a full grid array PBGA. A detailed examination of microstructure was performed at each step of the rework process, as highlighted in Figure 6. The influence of each rework step on mirrored and adjacent components was examined. The analysis focused on joint integrity, general defects, and microstructural changes such as intermetallic type and thickness, phase distribution and grain size.

### As-Received Component Solder Joint Characterization

The microstructures of as-received BGA components are shown in Figures 8a through 8d. Although both the  $\mu$ BGA and PBGA had SAC305 solder balls, the microstructure, composition, and intermetallic types after ball attachment were quite different.

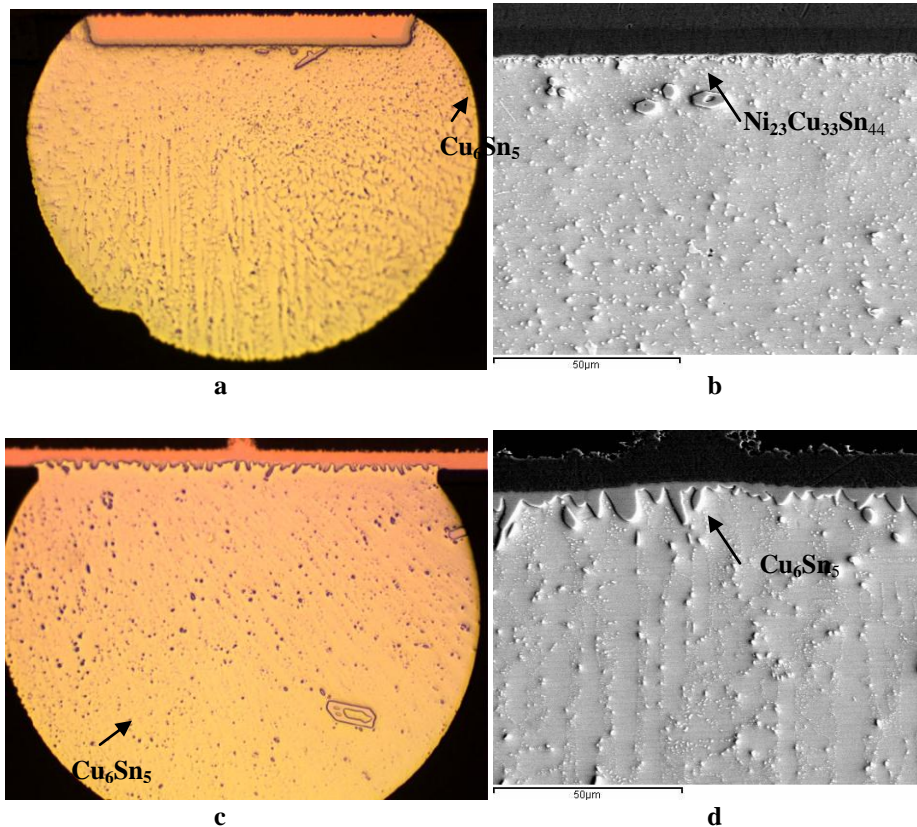


**Figure 8. Microstructure of As-Received  $\mu$ BGA (a, b) and PBGA (c, d): a: 200X; b: SEM 1000X; c: 200X; d: SEM 1000X**

The intermetallic reaction layer formed between ENIG finished pads of the  $\mu$ BGA and the SnAgCu solder ball contained 25.1 at. % Ni, 33.1 at. % Cu, and 41.9 at. % Sn (Table 3) and was found to be a ternary compound. The existence of this compound in a SnNiCu system was shown by Obendorff in 2001 [5] and was confirmed by L. Snugovsky et al [6] in 2005. As shown in [6], this ternary compound corresponds to the formula  $\text{Ni}_{23}\text{Cu}_{33}\text{Sn}_{44}$ . The intermetallic reaction layer was thin and did not exceed 1  $\mu\text{m}$  (Table 3).

The intermetallic layer of the PBGAs at the copper substrate pad was much thicker (Figure 8) with an average thickness of 5  $\mu\text{m}$ . It had a cellular structure with some spikes protruding into the bulk solder up to 8  $\mu\text{m}$ . The composition is shown in Table 3 and corresponds to the  $\text{Cu}_6\text{Sn}_5$  formulation.

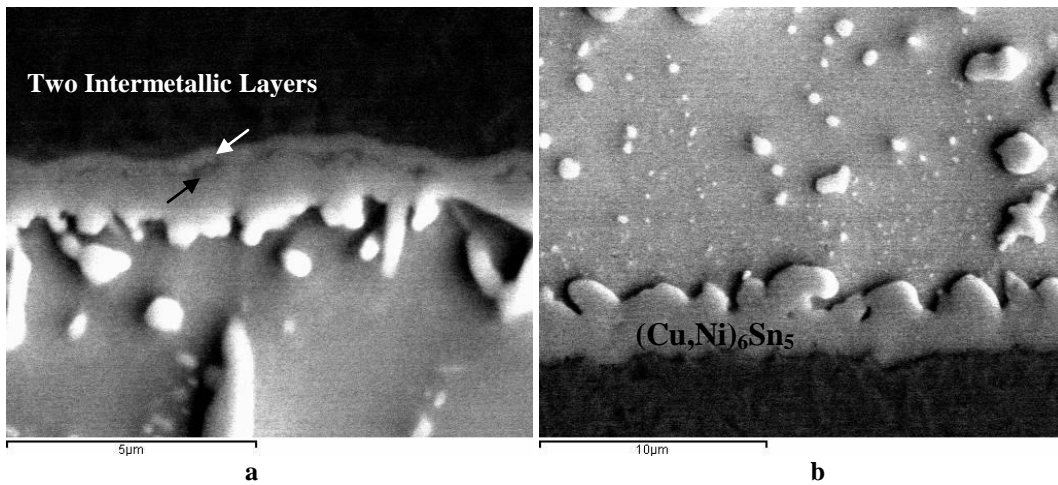
The microstructure of both the  $\mu$ BGA and PBGA (Figure 8) contained primary-like Sn dendrites and Sn+ $\text{Ag}_3\text{Sn}$ + $\text{Cu}_6\text{Sn}_5$  eutectic within the interdendritic spaces. The primary  $\text{Cu}_6\text{Sn}_5$  hexagons (which are hollow) were also present in both components. In the case of the PBGA, there were more  $\text{Cu}_6\text{Sn}_5$  particles and they were larger in size. This indicated a higher Cu content within the PBGA solder ball. The EDX analysis showed that  $\mu$ BGA balls contained 2.99%Ag and 0.55%Cu, which corresponded with a SAC305 sphere composition. The PBGA balls contained 3.1%Ag and 1.0%Cu that was a result of Cu dissolution during sphere attachment. The reduction of Cu pad thickness is also visible in Figure 8c.

**Table 3. Intermetallic Characteristics of As-Received, Assembled, and Reworked Components**

IMC	Thickness, $\mu\text{m}$	Composition						Formula	
		Cu		Ni		Sn			
		W %	At %	W %	At %	W %	At %		
Virgin $\mu\text{BGA}$	0.6	24.6	33.1	17.2	25.1	58.2	41.9	$\text{Ni}_{23}\text{Cu}_{33}\text{Sn}_{44}$	
Virgin PBGA	2.3	40.8	56.3	N/A	N/A	59.2	43.7	$\text{Cu}_6\text{Sn}_5$	
Primary attached $\mu\text{BGA}$	component	1.0	26.9	33.8	20.0	28.3	54.2	37.9	$\text{Ni}_{23}\text{Cu}_{33}\text{Sn}_{44}$
	board	3.0	36.3	50.6	2.4	3.6	60.3	45.0	$(\text{Cu},\text{Ni})_6\text{Sn}_5$
Secondary reflowed mirrored $\mu\text{BGA}$	component	1.2							$\text{Ni}_{23}\text{Cu}_{33}\text{Sn}_{44}$
	board	3.6							$(\text{Cu},\text{Ni})_6\text{Sn}_5$
Reworked $\mu\text{BGA}$	component	1.7	23.4	31.3	18.9	29.2	57.7	41.3	$\text{Ni}_{23}\text{Cu}_{33}\text{Sn}_{44}$
	board	6.4	39.7	54.3	2.0	3.0	58.3	42.7	$(\text{Cu},\text{Ni})_6\text{Sn}_5$
Reworked PBGA	component	2.5							$\text{Cu}_6\text{Sn}_5$
	board	2.8							$\text{Cu}_6\text{Sn}_5$

**As-Assembled SMT Reflowed Joints**

When assembled to the copper/OSP surface finish board during SMT primary attachment reflow processing, the  $\mu\text{BGA}$  microstructure underwent some changes. Two layers of intermetallic on the component side were visible under SEM at high magnification (Figure 9a). Also, long spikes grew from the previously flat intermetallic interface (Figure 9b). The composition of the two intermetallic layers was the same and similar to the as-received component (Table 3). The two layered structure may be explained by partial intermetallic dissolution during reflow followed by precipitation at the cooling stage, which resulted in a boundary formation in the intermetallic layer. The board side intermetallic was a  $\text{Cu}_6\text{Sn}_5$  type with some Cu atoms substituted by Ni (Table 3).

**Figure 9. Microstructure of SMT Primary Attached  $\mu\text{BGA}$ , SEM: a – Component Side; b –Board side**

The intermetallic layers of the bottom side  $\mu\text{BGA}$  components that reflow a second time during top side component rework were slightly thicker (Table 3). The thickness increased from 1 – 1.2  $\mu\text{m}$  and 3 – 3.6 $\mu\text{m}$  at the component and board sides respectively. The intermetallic compositions and types were the same as in primary attached joints (Table 3). There was no significant difference within the bulk microstructure as well.

### Hot Gas Reworked Joints

Reworked  $\mu$ BGA joints showed different intermetallic morphology, thickness and solder microstructure (Figure 10) than that of as-assembled joints. The intermetallic formed at the component side was slightly thicker than in primary attachment reflowed joints (1.0  $\mu\text{m}$ , 1.2 $\mu\text{m}$ , and 1.7  $\mu\text{m}$ , respectively) as shown in Table 3. Similar to the primary attached joints, two layers of intermetallic were detectable at the component side. Both were the  $\text{Ni}_{23}\text{Cu}_{33}\text{Sn}_{44}$  type.

The board side intermetallic layer of reworked  $\mu$ BGAs was more than two times thicker than in primary attachment  $\mu$ BGAs (Table 3). It was determined to be a  $\text{Cu}_6\text{Sn}_5$  type with some Ni atoms incorporated within the structure. Solid at the base on the Cu pad, the intermetallic layer turned into the lace-like structure closely resembling the bulk solder (Figure 10b). This intermetallic layer morphology was common for reworked BGA solder joints integrating NiAu on the component side and Cu on the PCB side (made available from surface finishes like OSP, Immersion Ag, or Immersion Sn).

The bulk solder joint microstructure of reworked  $\mu$ BGAs was also different from primary attachment top side and double reflowed bottom side joints (Figure 11). The microstructure also consisted of primary-like Sn dendrites and Sn+Ag<sub>3</sub>Sn+Cu<sub>6</sub>Sn<sub>5</sub> eutectic within the interdendritic spaces, but with Sn dendrites having a defined orientation and the larger dendritic arms. There were primary Cu<sub>6</sub>Sn<sub>5</sub> particles that were often attached and were close to the component side intermetallic layer (Figure 10a). The content of Cu in the bulk solder exceeded that of an as-received component by a factor of 2.6 (Figure 12) as a result of the Cu dissolution from the board side Cu pad. The Ag content was also slightly higher and will be discussed later in this paper.

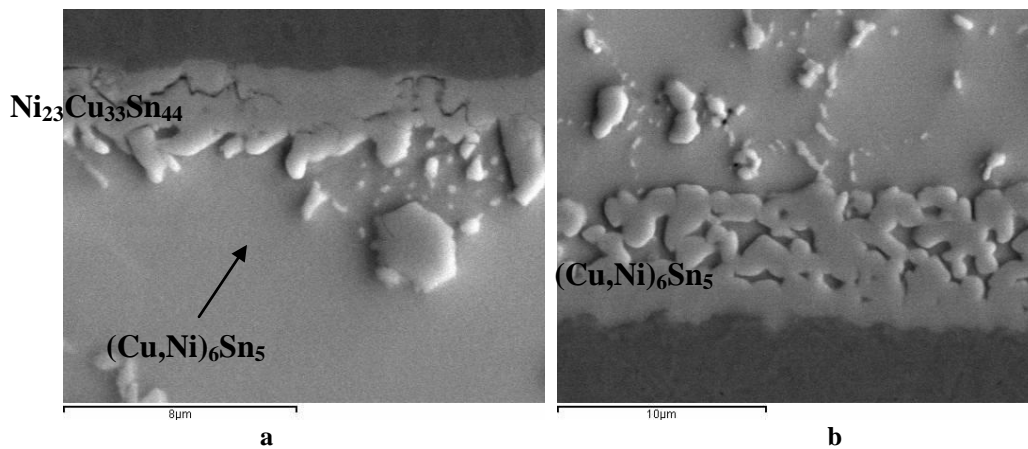


Figure 10. Microstructure of Reworked  $\mu$ BGA, SEM: a – component side, b –board side

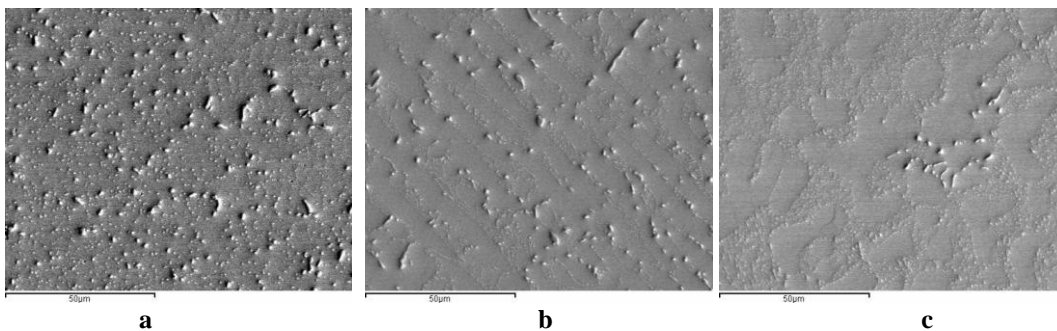
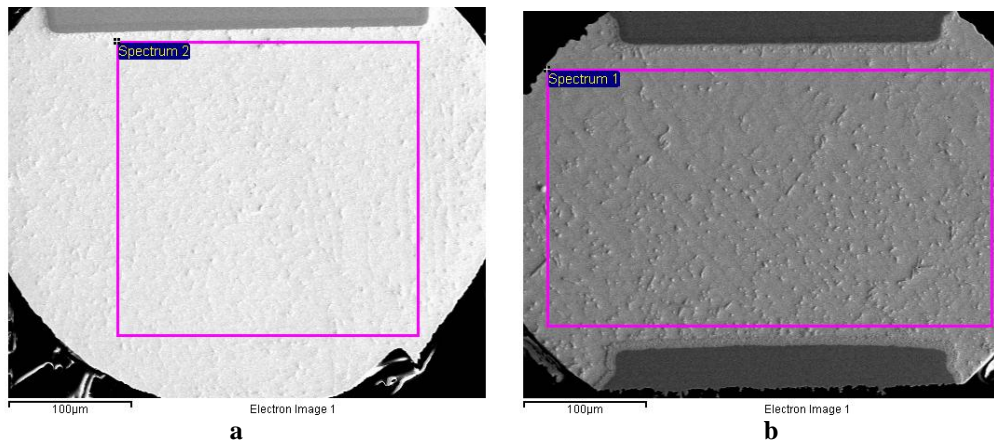


Figure 11. Microstructure of a Centre Ball from a Primary Attached  $\mu$ BGA (a), a Reworked  $\mu$ BGA

(b), and Reworked PBGA, (c) SEM 1000X



**Figure 12.** Microstructure and Composition of an Unassembled (a) and reworked (b)  $\mu$ BGA, SEM, 300X

Virgin $\mu$ BGA			Reworked $\mu$ BGA		
Element	Weight %	Atomic %	Element	Weight %	Atomic %
Cu	0.55	1.01	Cu	1.42	2.61
Ag	2.99	3.27	Ag	3.17	3.44
Sn	96.46	95.72	Sn	95.41	93.96

The intermetallic characteristics and microstructure of the reworked PBGA is shown in Table 3 and Figure 13. The  $\text{Cu}_6\text{Sn}_5$  type with the same composition, microstructure, and thicknesses was formed on the component and board sides. The morphology of both component and board layers were completely different from those found within the  $\mu$ BGAs (Figure 10). The intermetallic layers found within the reworked PBGAs did not have a lace-like or layered structure. Instead, they were dense and had a cellular structure. This difference indicates different behaviour of the  $\text{Ni}_{23}\text{Cu}_{33}\text{Sn}_{44}$  and  $(\text{Cu},\text{Ni})_6\text{Sn}_5$  when compared to  $\text{Cu}_6\text{Sn}_5$  during dissolution followed by precipitation during the rework process. As shown in Figure 11, the bulk solder joint microstructure of PBGAs was coarser and the proportion of eutectic was higher than found within the  $\mu$ BGAs.

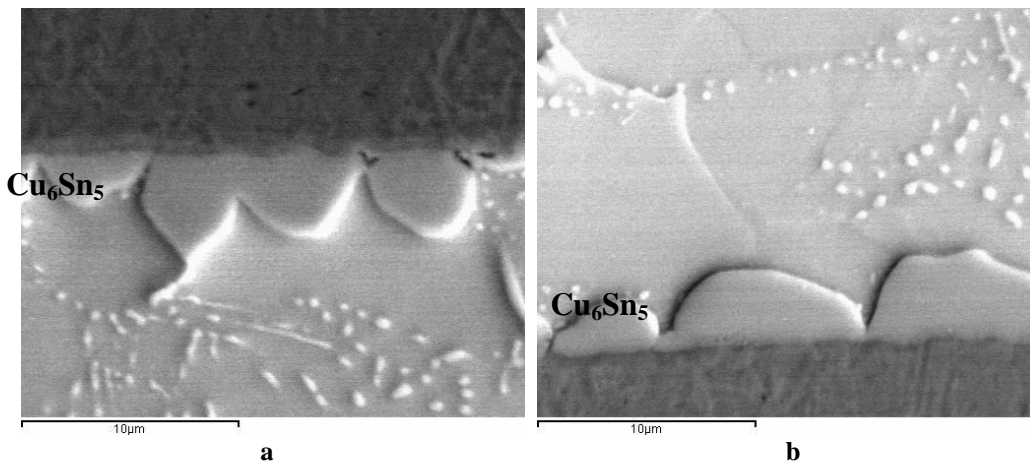


**Figure 13.** Microstructure of reworked PBGA, SEM, 5000X: a – component side; b –board side

The rework microstructures discussed above were obtained after the optimization of the rework processes. The criteria for rework parameter optimization were proper solder joint formation as well as defect-free mirrored component solder joints after rework.

### Defects within Mirrored Component Solder Joints

The defects found within mirrored solder joints detected *prior to process optimization* are shown below in Figure 14. The mirrored solder joints often had irregular shapes (Figure 14a, b). Also, voids or partial separation between the solder and the intermetallic layer were present in mirrored BGAs located under the reworked location (Figure 14c, d). These defects were not observed in SnPb solder control samples. Detailed analysis revealed that the separation propagated through the SnAgCu ternary eutectic phases accumulating at the board side. The separation had a dendritic shape. As shown in Figure 14d, it follows the eutectic boundary between the board surface and dendritic arms. The alloy's pasty range was determined to be the reason for this separation and irregular shape.

During cooling of SnAgCu alloys after reflow, solidification began with the formation of primary  $\text{Ag}_3\text{Sn}$  or  $\text{Cu}_6\text{Sn}_5$  depending on solder composition. Next, Sn nucleation occurred. The Sn phase grew in a dendritic shape towards the hot board side. Finally, the liquid crystallized as a binary system ( $\text{Sn}+\text{Ag}_3\text{Sn}$  or  $\text{Sn}+\text{Cu}_6\text{Sn}_5$ ) and then ternary eutectic ( $\text{Sn}+\text{Ag}_3\text{Sn}+\text{Cu}_6\text{Sn}_5$ ) within interdendritic spaces. The last portion of liquid with the lowest melting temperature solidified at the board side. The melting temperature of the ternary eutectic in SnAgCu solder alloys was approximately  $217^\circ\text{C}$ . Any additional constituents resulting from dissolution of the substrate material, such as Au in the joints with NiAu finished components, segregated in the last liquid to freeze and reduce the eutectic temperature even further. The presence of a quaternary  $\text{Sn}+\text{Ag}_3\text{Sn}+(\text{Cu},\text{Ni})_6\text{Sn}_5+\text{AuSn}_4$  eutectic was detected within the analyzed assemblies (Figure 15a). The DSC curve of an as-assembled solder joint is shown in Figure 15b. It revealed that melting may begin at a temperature as low as  $212.5^\circ\text{C}$ . Narrow liquid layers form between the Sn dendrites and the intermetallic layer /solder interface at the board side. Sliding and opening between the Sn grains and the intermetallic layer / solder interface under internal stresses help to explain the observed irregular solder joint shapes, voids, and separations.

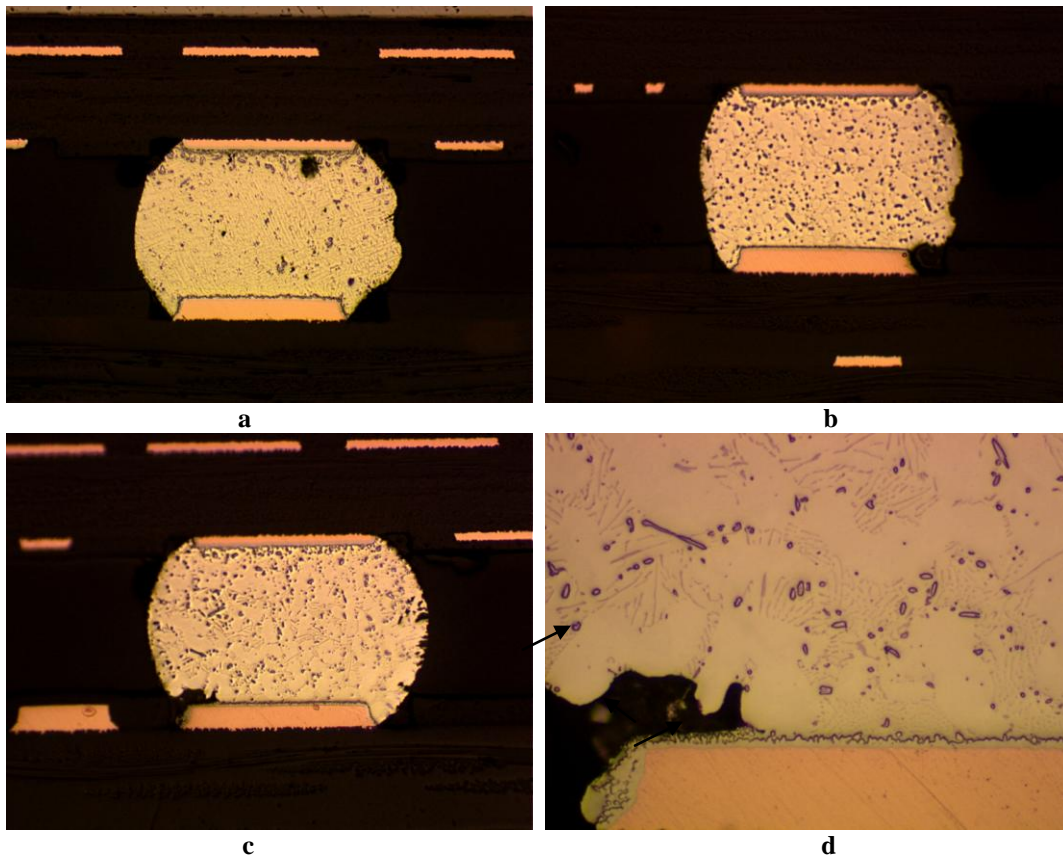


**Figure 14.** Defects of Mirrored  $\mu\text{BGAs}$  after Topside Rework: a, b, c – 100X; d – 400X

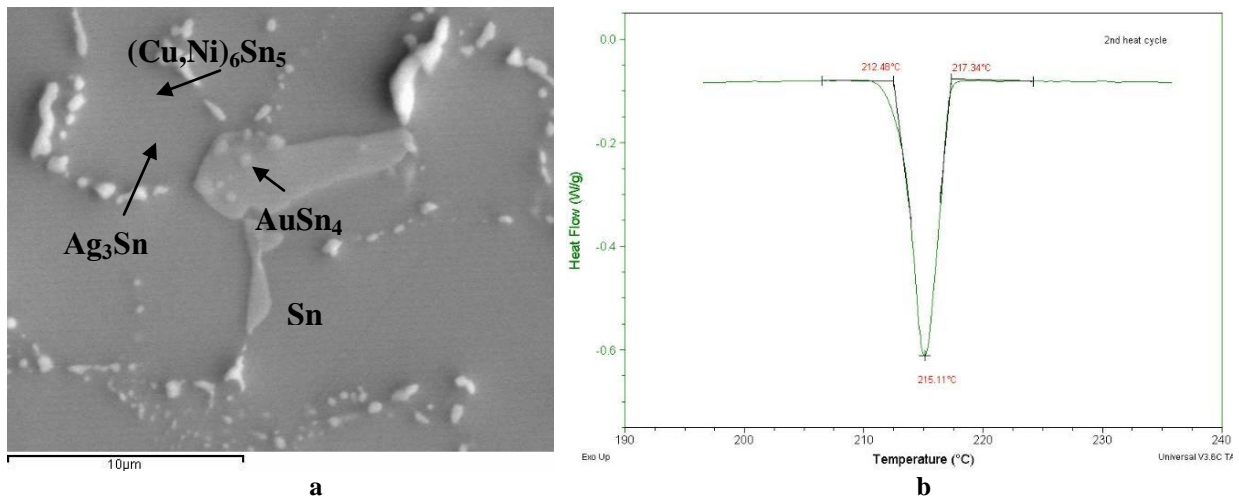


**Figure 15.** Microstructure of the Low Melting Eutectic (a) and DSC characterisation of melting  $\mu\text{BGA}$  joints

### Analyses of Rework Steps

To further understand the final microstructure of mirrored BGA solder joints after top side rework operations, metallurgical analysis after each process step was performed. During component removal the bulk solder melted. The intermetallic layer at the board side as well as single primary intermetallic  $\text{Cu}_6\text{Sn}_5$  particles started dissolving into the liquid solder. This resulted in intermetallic thickness reduction (Table 4) and the changing of the shape of the primary crystals. A significant amount of solder was still attached to the board pad after original component removal (Figure 16).

IMC		Thickness, $\mu\text{m}$
Removed $\mu\text{BGA}$	board	2.6
Removed and redressed	board	4.6
Mirrored $\mu\text{BGA}$ under removed site	component	1.0
	board	3.1
Mirrored $\mu\text{BGA}$ under removed and redressed site	component	1.0
	board	3.2

**Table 4.** Intermetallic Characteristics in Different Steps of  $\mu\text{BGA}$  Rework

Component removal caused the most significant changes in microstructure of mirrored BGAs. The area of the mirrored solder joint closest to the board was shown to surpass the alloy's melting temperature. In a semi melted stage, microstructure coarsening and separation occurred. The separation propagated through the solder grain boundaries between the intermetallic layer and the bulk solder. This observation may occur through the intermetallic layer because of the greatly reduced strength of the intermetallic at the temperature near the melting point and increased internal stresses. This defect is quite dangerous because it may be aggravated during thermal cycle exposures (Figure 17). The thickness of the intermetallic layers at both the component and board sides were not affected and were similar to SMT reflowed primary attachment joints.

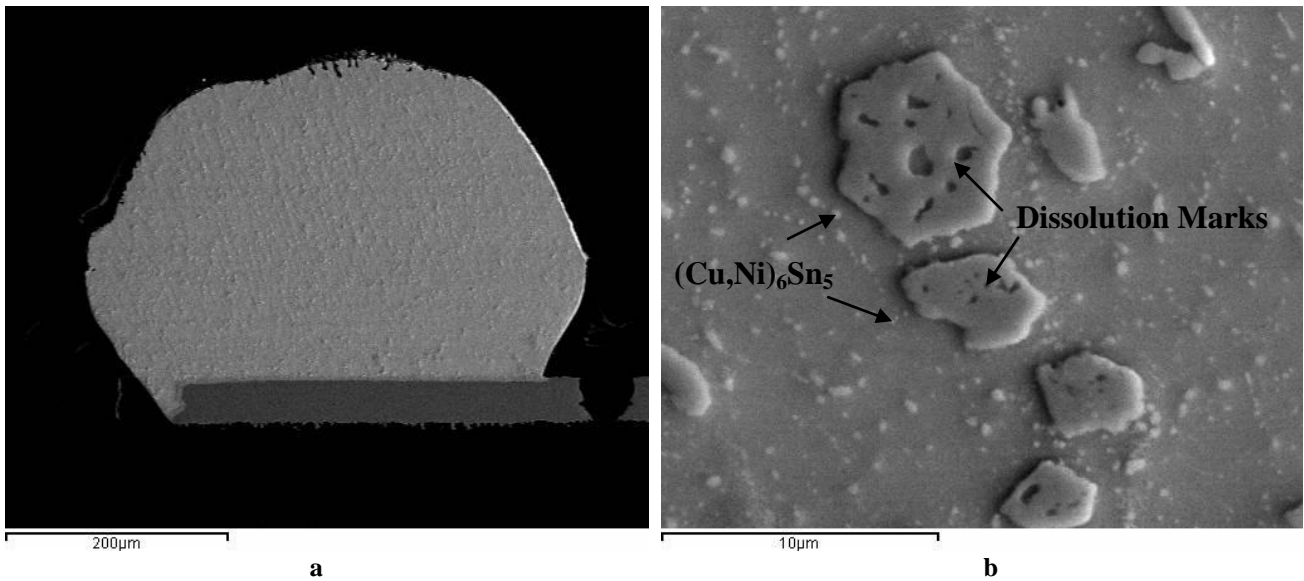


**Figure 16.**  $\mu$ BGA location after component removal: a – 200X; b - Microstructure of partially dissolved  $\text{Cu}_6\text{Sn}_5$  particles

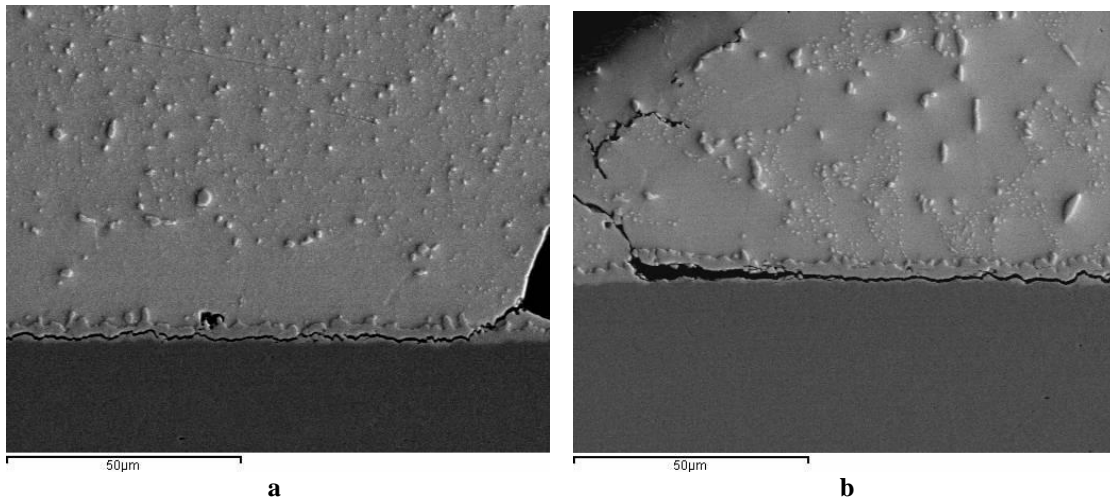


**Figure 17.** Mirror  $\mu$ BGA under removed component, SEM, 1000x: a – after component removal; b – ATC

During the redress step, most of the solder left after component removal was consumed by using Cu solder wick. The top view under the SEM is shown in Figure 18. The pads look flat compared to the previous component removal stage of rework (Figure 18a, b). EDX analysis indicated that in addition to the  $\text{Cu}_6\text{Sn}_5$  area - black spots (solder with very high Ag content – 8.8 to 18%) were present. The microstructure of a cross-sectioned pad after site redressing is shown in Figure 8d. Some solder still remained on top of the intermetallic layer. This solder contained many  $\text{Ag}_3\text{Sn}$  intermetallic particles that caused a shift in its composition from the near eutectic to off-eutectic. This accumulation of the  $\text{Ag}_3\text{Sn}$  intermetallic particles resulted in higher Ag content within reworked solder joints, as previously discussed. There was no change observed in intermetallic thickness after this process step.

Mirrored components, after redressing the rework site, demonstrated similar separation and shrinkage defects that were shown before in the samples after component removal. These defects may be inherited from the previous stage of rework, or created additionally (Figure 19).

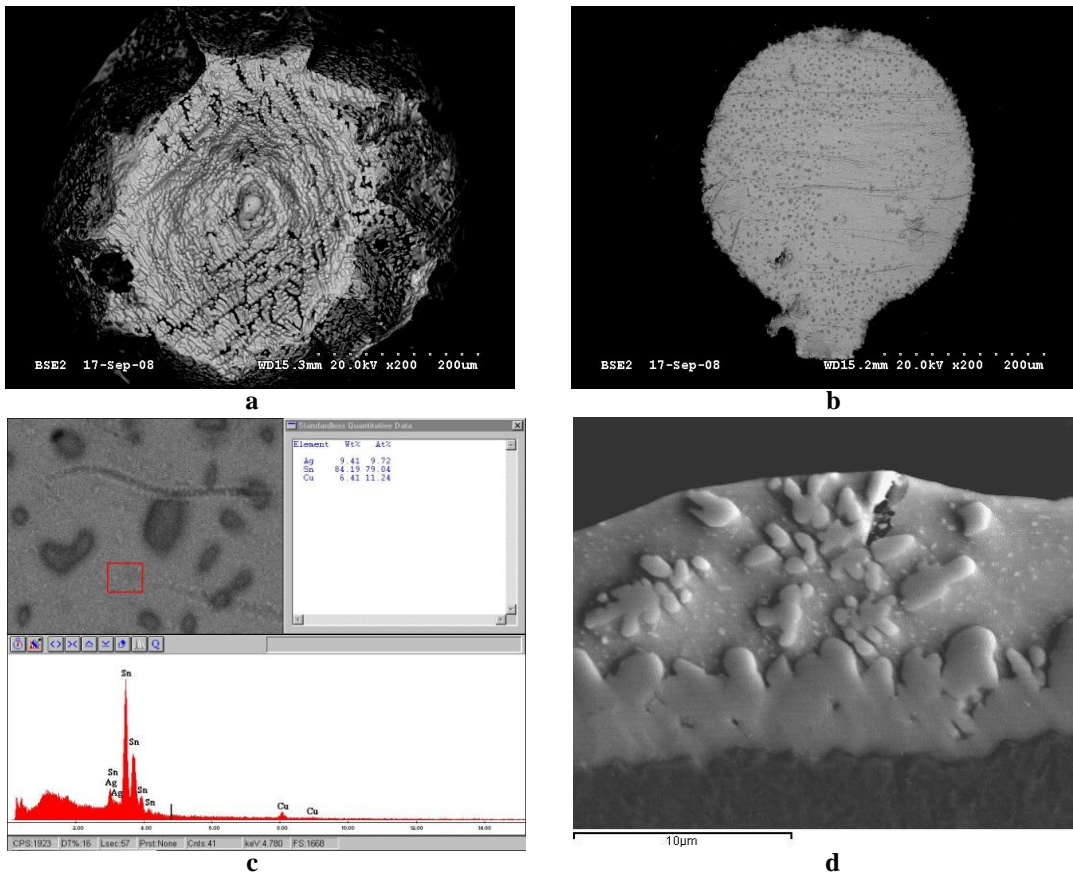


**Figure 18.** SEM Photos of Pads after Component Removal (a) after Removal and Redressing, (b) Residual Solder Composition, (c) Cross Sectional Composition, (d) Final Microstructure

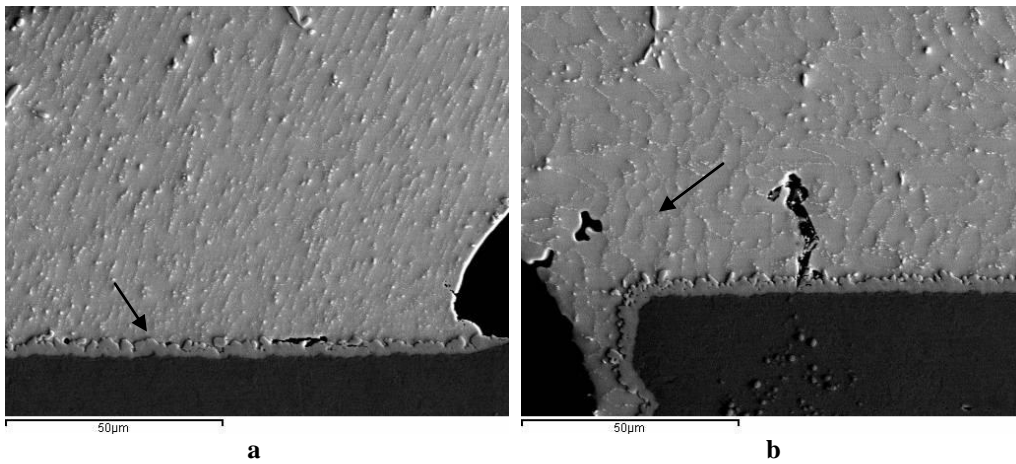


**Figure 19.** Mirrored µBGA under reworked component, separations caused by partial melting, SEM, 1000x

During the final hot gas rework step; new component attachment reflow may be achieved using one of several options including: (a) using a traditional SnPb assembly approach; avoiding mirrored BGA secondary reflow; (b) rework that allows partial melting of mirrored BGA solder joints or (c) rework allowing fully melted joints of mirrored BGAs.

As discussed, option (a) which prevents the melting of mirrored BGA solder joints may not provide sufficient heat to thermally activate flux that has wicked under mirrored BGAs. Option (b) which allows partial melting may aggravate the defects from the removal and redressing rework process steps discussed within this paper. If partial melting of the Sn occurs near the intermetallic layer / bulk solder interface, defects that look like tiny cracks may be produced as shown in Figure 20.

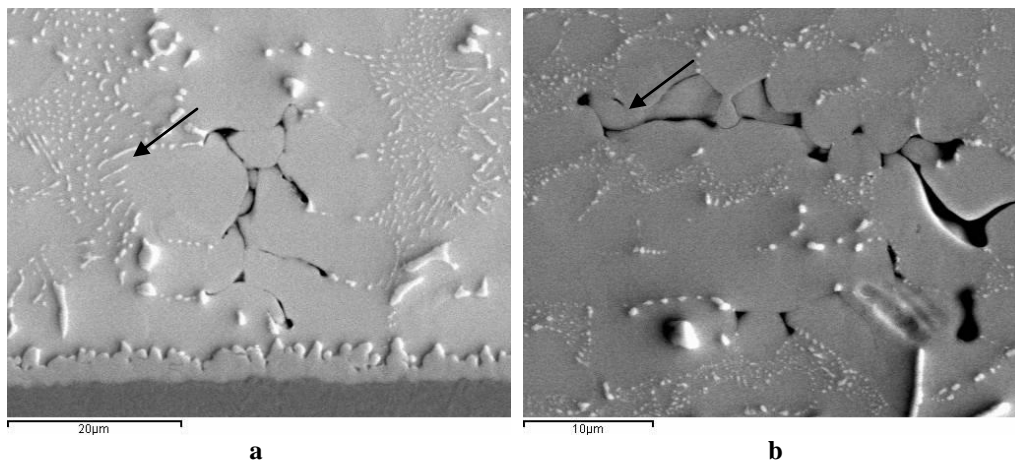
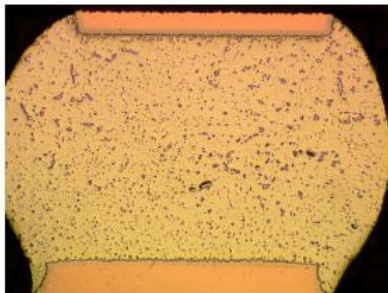


**Figure 20.** Mirrored  $\mu$ BGA under Reworked (a)  $\mu$ BGA and (b) PBGA, separations caused by partial melting, SEM: A – 2000X: b – 3000X

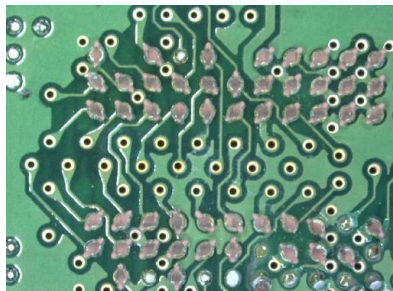
Once option (c) was employed, reflow profiles for both  $\mu$ BGA and PBGA allowed joints to form with a good shape and microstructure (Table 3 and Figures 9 – 13). The mirrored components were fully melted and solidified again. These joints were free of defects.

#### Optimized Process Construction Analysis

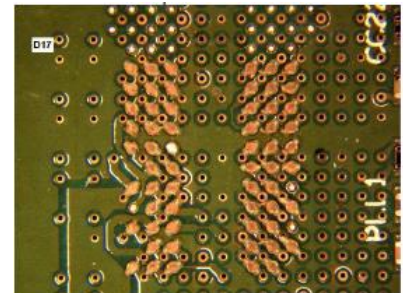
Construction analysis showed that resultant mirrored BGAs had excellent bulk solder joint collapse and had well-formed IMC layers at the PCB and component side interfaces. In addition to the excellent metallurgical structure observed, significant process improvements reduced flux residue and the amount of flux pooling down via structures; reducing the risk of dendritic growth shorting. Example final structures are shown in Figure 21.



Well formed joints; good IMC



Die & Pry performed well



Reduction in flux pooling

**Figure 21.** Backside Flux Pooling eliminated with Excellent Solder Joint Formation and Collapse

#### Thermo Mechanical Reliability Testing Trials

Using optimized profiles and allowing mirrored BGAs to fully reflow during top side rework operations, test cards were subjected to a series of thermo mechanical reliability test environments. Six different tests were conducted including Temperature, Humidity & Bias Testing (TH&B), Accelerated Thermal Cycling (ATC) 0-100°C for 1 cycle per hour, High Temperature Storage (HTS) 125°C for 1000 hours, Drop Testing, combination Torque / Shock / Vibration / ATC testing, and Time Zero Construction Analysis. Prior to all test starts test cards were subjected to thermal ship shock (TSS) conditions.

In summary, Table 5 shows that test assemblies built and reworked allowing mirrored BGAs to fully reflow passed all six thermo mechanical test protocols with no failures.

**Table 5.** Test Matrix and Results for Fully Reflowed Mirrored BGAs

Cell	Assembly Type	Reliability Test	Test Result
1	Forced Rework	TSS / TH&B	PASS
2	Forced Rework	TSS / ATC 1200 cycles	PASS
3	Forced Rework	TSS / HTS	PASS
4	Forced Rework	Drop Test / ATC 250 cycles	PASS
5	Forced Rework	Torque / Shock / Vibration / ATC 250 cycles	PASS
6	Forced Rework Primary Attachment	Time Zero Construction Analysis	PASS

**Microstructure after ATC**

In order to evaluate the thermal mechanical reliability, the test cards with reworked  $\mu$ BGA and PBGA using optimized rework profiles were thermal cycled at 0°C to 100°C. The ATC profile had a dwell time of about 15 minutes at both high and low temperatures, with 15 minutes ramps up and down. The test duration was 1200 cycles. All cards passed the test without any failures. The microstructure after cross-section is shown in Figure 22. It was slightly coarser than before ATC. The maximum damage that was found after 1200 cycles was a small crack in the PBGA (Figure 22d). The crack was initiated at the board side and penetrated into the solder joint along the intermetallic/solder interface for about 15 $\mu$ m.

The microstructure of mirrored joints after ATC was also slightly coarsened and the intermetallic thickness was increased to 4 $\mu$ m and 1.4 $\mu$ m at the board and component sides, respectively. Again, there were no cracks found in mirrored joints.

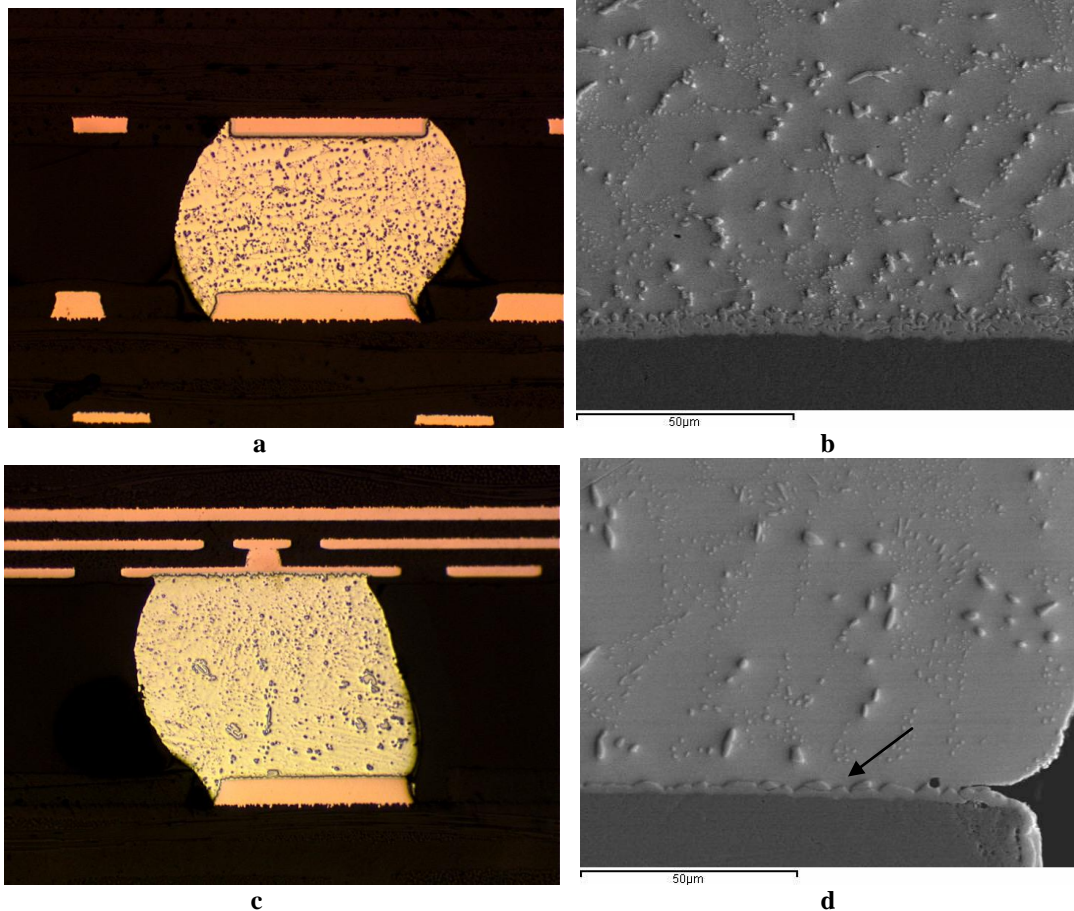


**Figure 22.** Reworked (a, b)  $\mu$ BGA and (d, c) PBGA after ATC: a – 100; b – SEM, 1000X; c – 100X; d – SEM, 1000X

## Summary and Conclusions

A migration to no-clean flux chemistry has accompanied the change to lead-free hardware assembly. Secondly, the use of mirrored BGA design points continues to grow in today's PCBA layouts, attempting to pack more I/O into smaller card formats.

As a result, changes to the hot gas rework process of PCBA designs with lead-free mirrored BGAs are required from traditional SnPb methods. A new material and process solution was developed and tested to yield excellent time zero quality and longer term reliability results. Changes to the flux chemistry, flux application, and flux control were made to mitigate dendritic growth and subsequent electromigration risks.

From a process perspective, increased thermocouple monitoring was implemented ensuring accurate measurement of the PCB, local temperature sensitive components, shielding of adjacent BGAs, and mirrored BGA times and temperatures. Lastly, a change in approach during hot gas rework reflow was implemented; allowing mirrored BGA solder joints to fully reflow, avoiding the SnAgCu pasty range.

There were many findings resultant from this work and are listed below within three categories; materials, rework process, and reliability / metallurgical conclusions.

## Materials

- Halide-free (L0) flux chemistry should be used for lead-free no-clean assembly and rework processing. This chemistry type reduces the risk of dendritic growth even when fluxes or residues are not properly thermally activated during primary attachment or rework processing. The use of L0 type fluxes helps to integrate process safeguards within volume manufacturing environments.
- The use of liquid flux during mirrored BGA hot gas rework is recommended over traditional tack flux formulations. Tack fluxes will often be smeared into open via structures during site redress, will wick down vias to a mirrored BGA location, and if un-activated, can lead to flux pooling and potential dendritic growth. A focus on flux control and application method is extremely important for mirrored BGA design rework processing.
- SIR or TH&B electromigration testing confirmation of all assembly materials should be conducted to assess dendritic growth risks of mirrored BGA constructions.

## Rework Process

- Mirrored BGA solder joints should be allowed to reflow during lead-free hot gas rework processing. The pasty range of the alloy must be avoided in order to minimize shrinkage void defects and to maximize the solder joint reliability. Higher processing temperatures during mirrored BGA rework also help to ensure that fluxes are fully activated under mirrored devices; in case small amounts of flux do wick down via structures during redress operations.
- An increased number of thermocouples should be used during hot gas mirrored rework profiling. Monitoring of the reworked BGA location, adjacent BGA joints, local TSCs, local PCB, and mirrored BGA locations is critical to ensure a robust and reliable process.
- Identification of temperature sensitive components nearby rework locations is critical. Local TSCs must be properly monitored to ensure temperature and time at temperature limitations are not exceeded during the rework operation. If violations do occur during the hot gas process, replacement of local TSCs is recommended using a hand iron.
- Same side adjacent component partial reflow during hot gas rework should be avoided via increased thermocouple monitoring and shielding when required.

## Reliability and Metallurgy

- Copper dissolution plays an important role in the reliability of reworked mirrored BGA solder joints. Mirrored BGA solder joints after the rework process can have up to 3X more copper wt% within each joint; thus creating the potential for reliability reduction of solder joints. Although it is advantageous to allow mirrored BGAs to fully reflow during top side rework operations, this copper dissolution observation suggests that there is an upper bound to acceptable temperature and time at temperature process windows. (Additional work is required to determine these limits).

- Due to dissolution of additional elements from surface finishes such as Au in the ternary composition of SnAgCu alloy systems, there is a depression of an offset melting temperature below 217°C. For the material combination used in this study melting has been shown to start as low as 212.5°C. If mirrored BGA solder joints approach this pasty range a liquid phase will develop allowing for shrinkage voids and phase separation to occur upon cooling. This observation supports the argument to avoid this pasty range completely and allow mirrored BGA solder joints to reflow during rework operations.
- Top side component removal during the hot gas rework process is the most damaging step for mirrored BGA reliability performance. During top side component removal, high temperatures can begin the onset of the quaternary eutectic liquid phase and lead to irregular solder joint shapes, shrinkage voids, and separations.

### **Acknowledgements**

The authors thank the following individuals for technical discussions and paper review: Marie Cole and Jim Wilcox from IBM, Thilo Sack and Prakash Kapadia from Celestica.

### **References**

- [1] *“Process Development with Temperature Sensitive Components in Server Applications”*, L. G. Pymonto, W.T. Davis, Matthew Kelly, Marie Cole, James Wilcox, Paul Krystek, Curtis Grosskopf. IBM Corporation. APEX 2008, Las Vegas, Nevada, USA. April 2008.
- [2] IPC J-STD-004, “Requirements for Soldering Fluxes”, Joint Industry Standard.
- [3] *“Surface Insulation Resistance Testing of Soldering Pastes and Fluxes”*, Renee Michalkiewicz, Janet Green, and Scott Opperhauser. Trace Laboratories. Pan Pacific Microelectronics Symposium, Kauai, Hawaii. February 2001.
- [4] *“Guide for Flux Selection in Modern Electronic Industry”*, Darlene R. Hug. Technical Services Laboratory, Alpha-Fry Technologies. July 2003.
- [5] “Lead-free solder systems: phase relations and microstructures”, P. J. T. L. Oberndorff. PhD Thesis, Technische Universiteit Eindhoven, the Netherlands, 2001.
- [6] “Phase Equilibria in the Sn-rich Corner of the Cu-Ni-Sn System”, L. Snugovsky, P. Snugovsky, D.D. Perovic and J.W. Rutter. *Materials Science and Technology*, vol.29, No 8, pp. 899 – 902, 2006.